J Mater Sci (2017) 52:13812–13828

Composites

Improving the interfacial property of carbon fiber/vinyl ester resin composite by grafting modification of sizing agent on carbon fiber surface

Weiwei Jiao[1], Wenbo Liu[1,*], Fan Yang[2], Long Jiang[2], Weicheng Jiao[2], and Rongguo Wang[2,*]

[1] School of Materials Science and Engineering, Harbin Institute of Technology, Harbin 150001, China
[2] Center for Composite Materials and Structures, School of Astronautics, Harbin Institute of Technology, Harbin 150080, China

Received: 15 June 2017
Accepted: 16 August 2017
Published online: 22 August 2017

ABSTRACT

The poor interfacial adhesion between carbon fibers (CFs) and vinyl ester resin (VE) has seriously hampered the application of CFs/VE composites. In this work, the interfacial adhesion was efficiently enhanced by grafting acrylamide with epoxy sizing agent on CFs surface. The grafting reaction was feasible according to the thermodynamic calculation. The optimal grafting condition was 80 °C for 10 min based on the kinetic investigation by differential scanning calorimeter. Surface morphology and surface composition of modified carbon fibers (MCFs) were characterized, which indicated that acrylamide was grafted successfully on CFs surface and the surface roughness was increased slightly. After grafting, the interface shear strength of MCFs/VE composites was significantly improved by 86.96% and the interlaminar shear strength was enhanced by 55.61% due to the covalent bonds in interphase and the toughening effect of sizing gent. Moreover, the static and dynamic mechanical properties of composites with different interfacial adhesion were measured, which further confirmed the effect of the grafting modification.

Introduction

Carbon fibers reinforced resin composite (CFRP), with superior strength-to-weight ratio, excellent mechanical and thermal stability and outstanding design ability, has become the first choice replacing metal materials for automobile lightweight. CFRP has been increasingly used in transportation due to the decline in carbon fibers (CFs) prices. Different with traditional aerospace field, automotive CFRP requires a short production cycle to meet the need of mass production of auto parts. That means a fast-curing resin should be selected, such as vinyl ester resins (VE). VE, a kind of thermosetting resin obtained by the reaction of epoxy resin with unsaturated organics, inherits the excellent mechanical property, high-temperature resistance and chemical resistance of former, and introduces the outstanding curing property and forming performance as unsaturated

Address correspondence to E-mail: liuwenbohit@163.com; wrg@hit.edu.cn

DOI 10.1007/s10853-017-1485-8

polyester resin [1]. However, VE is nonreactive with epoxy sizing agent on carbon fiber surface, which may lead to the lack of chemical bonds in interphase and the poor interfacial adhesion performance for CFs/VE composites [2]. This weakness of the interface has limited the practical application of the composite significantly [3].

The interfacial connection plays the most important role in the overall performance of CFRP under the given carbon fiber and resin matrix [4, 5]. In order to improve the interfacial properties of CFRP, extensive researches have been devoted to the surface treatment of CFs. Untreated CFs is difficult to form a stable connection with resin matrix on account of its highly stable, nonpolar and smooth graphitic surface [6, 7]. These surface treatments, including sizing process [8], grafting [9], oxidation [10], electrochemical method [11], plasma treatment [12, 13], introduced polar functional groups on the CFs surface to improve the surface energy [14] and/or increased the surface roughness of the fiber [15, 16]. A novel "coupling agent" *N*-(4-amino-phenyl)-2-methyl-acrylamide was synthesized and grafted on oxidized CFs surface by Zhang et al. [17]. After grafting, the interfacial shear strength between CFs and VE improved by 90.53%, while the flexural strength of composite increased only by 19.4%. The author believed this disparity was attributed to the dominant role of CFs to the flexural strength. However, the acid oxidation treatment may lead to the strength decline of CFs. Moreover, CFs will be easily fluffed and broken without sizing process. Both of these reasons can cause the inconsistency of the increase amplitude between flexural strength and interfacial shear strength. Therefore, vinyl functionalization on oxidized carbon fiber surface may not be an ideal interface modification method to improve the overall performance of the composites.

Sizing process is another CFs surface modification method which can effectively improve the interface property of the composite material. The main ingredients of sizing agent are usually polymers, most of which are epoxy resin. Xu et al. [18] believed that the residual stress in interfacial phase caused by cure volume shrinkage of vinyl ester resin would decrease interfacial shear strength (IFSS) between fiber and matrix. The epoxy sizing on the fiber surface could counteract the cure volume shrinkage of vinyl ester resin and relax the residual stress by swelling in the matrix. Broyles et al. [19–21] sized CFs with different thermoplastic sizing agent to improve the fatigue resistance of CFs/VE composites. However, negligible differences in the shear strength, flexural strength and static compressive strength were observed for the different interphase agents. Verghese et al. [22] managed to build connection between molecular relaxation behavior and interfacial adhesion properties of CFs/VE composites. The CFs was coated with different thermoplastic sizing agent. Nevertheless, neither epoxy sizing agent nor thermoplastic sizing agent can chemically cross-link with the vinyl ester resin matrix.

In this work, vinyl functionalization was performed directly on epoxy sizing agent on CFs surface other than unsized or oxidized CFs surface. In principle, the grafting modifier could be any organic molecules composed of unsaturated double bonds and functional groups which can react with epoxy sizing agent. The aqueous solution of acrylamide (AM) was used herein. After modification, CF was covalently linked with VE by AM molecule like a bridge, as shown in Fig. 1. This interfacial modification method integrated the advantages of grafting and sizing process and avoided the damage in carbon fibers during oxidation process. Carbon fibers reinforced VE composites were prepared. Interfacial sheer strength, interlaminar shear strength, dynamic mechanical properties and static mechanical properties of different composites were tested to investigate the effect of interface modification.

Experimental

Materials

Polyacrylonitrile (PAN)-based T700 SC CFs (12 K) investigated in this study was manufactured by Toray Company, Japan. Vinyl ester resin diluted by styrene was purchased from Shanghai Fuchem Chemical Co., Ltd, Shanghai, China, with the trade name of P104-02. All other chemicals, such as acrylamide (AM), tert-butyl peroxybenzoate (TBPB), hydroquinone, zinc stearate, active magnesium oxide (MgO) and acetone were purchased from the Aladdin Chemistry Co., Ltd, Shanghai, China, and used as received without further purification.

Thermodynamics and kinetics of the grafting reaction

The thermodynamics of the reaction between AM and epoxy sizing agent was simulated using Accelrys®

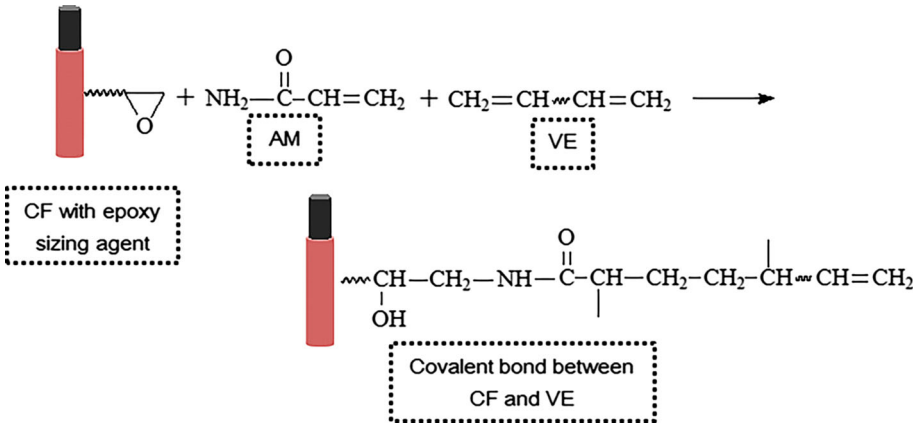

Figure 1 Schematic diagram of bridging between CF and VE matrix in the interface area.

Materials Studio® V7.0 software. The epoxy sizing agent used in the simulation was E44 epoxy resin. Fig. S1 shows the chemical formulas and models of AM, E44 and their reaction product (UE). It is noteworthy that all of the following simulation processes were performed on the three molecules separately. A geometry optimization was carried out using smart algorithm to partially relax the molecular structures and minimize their total energy. Then the quench molecular dynamics was run using an NVE ensemble (constant number of atoms, *N*; constant volume, *V*; and constant energy, *T*) at 600 K with a time step of 1.0 fs for 100 ps. The condensed-phase optimized molecular potentials for atomistic simulation studies (COMPASS) force field developed by Sun [23] was used for this study. A quench or geometry optimization was performed every 5000 steps and 21 conformations were sampled. Among the conformations, the one with the lowest energy was selected for further geometry optimization and vibrational analysis calculation by density functional theory (DFT). BLYP potential based on generalized gradient approximation (GGA) was used as exchange–correlation functional in calculations. The finite temperature-corrected values E^{T}_{Tcorr} for free energies of the three molecules were calculated from data contained in output document, and the ΔG value for the reaction can be calculated using the following formula:

$$\Delta G^{T}_{\mathrm{reaction}} = E^{T}_{\mathrm{TCorr}}(\mathrm{product}) - E^{T}_{\mathrm{TCorr}}(\mathrm{reactant}) \qquad (1)$$

The kinetics of the reaction was experimentally studied. Firstly, the carbon fibers were refluxed in acetone at 75 °C for 48 h, then washed with deionized water repeatedly and dried under vacuum at 100 °C for 4 h to obtain epoxy sizing agent and desized CFs (DCFs) [8]. Then the epoxy sizing agent was dissolved in ethanol and mixed with acrylamide at a mass ratio of 1:5 for differential scanning calorimeter (DSC) measurement at elevated temperature (5 °C/min, from 20 to 150 °C) and constant temperature (80 °C, based on the measurement result at elevated temperature). In addition, the Fourier transform infrared (FTIR) spectrums of sizing agent and the mixture after reaction were measured to characterize the changes in functional groups of sizing agent before and after reaction.

Surface treatments of carbon fiber

The above-mentioned DCFs were treated by a 3:1 (v/v) mixture of concentrated H_2SO_4/HNO_3 at 70 °C for 2 h. After modification, the carbon fibers were thoroughly washed with deionized water, and then dried at 50 °C for 24 h to obtain oxidized CFs (OCFs).

The grafting process of acrylamide on CFs and DCFs surface can be carried out continuously, as illustrated in Fig. S2. In this study, carbon fibers were immersed in beakers containing aqueous solution of acrylamide with mass fractions of 0.5, 1.0 and 1.5%, respectively. Plastic film was used to seal the beakers and ultrasonic vibration was used to speed up the grafting reaction. After modification, the carbon fibers were washed with deionized water to remove excess acrylamide on fibers surface and then dried in an oven at 105 °C (labeling as MCFs and MDCFs). The temperature of grafting modifiers and the modification time were determined by the DSC test results.

Preparation of composite materials

Micro-droplet composites for interfacial sheer strength (IFSS) test were prepared using single fiber.

The single fiber was strained and fixed on a metal framework, and then the vinyl ester resin was uniformly dropped on the fiber to form micro-droplets. After that, the samples were cured as same as the conditions in the literature [17].

Multifilament composites for comparing the tensile properties of CFs, OCFs and MCFs were prepared according to ASTM D4018-99 standard. The carbon fibers bundle was impregnated with epoxy resin manually and then attached to a rack to hold it under tension during consolidation under the same conditions as the micro-droplet composites. The resin content was controlled at about 50% by weight. End tabs were applied to the impregnated and consolidated specimens. The distance between tabs was 150 mm.

The carbon fibers reinforced vinyl resin composites were prepared by compression molding forming as sheet molding compound (SMC) [24]. The difference was that the chopped carbon fiber in SMC was replaced by unidirectional carbon fiber or plain weave fabric. Main ingredients and formulations of the resin paste are described in Table 1. The SMC prepreg was thickened at 50 °C for 48 h, and then cut and stacked in a mold preheated to 140 °C. Clamped the mold and pressurized to 5 MPa for 5 min at preheated temperature.

Characterization

Raman microscope (Renishaw inVia) and X-ray photoelectron spectroscopy (XPS, PHI5700) were used to evaluate the molecular and chemical structures of pristine CFs, DCFs and grafted CFs. For XPS, functional groups were assigned using reported C1*s* and N1*s* chemical shifts in various organic compounds, and the relative amounts of these groups were estimated from respective areas of fitted Gaussian–Lorentzian curves. Surface morphologies of CFs before and after grafting were characterized with a Quanta 200 FEG scanning electron microscope (SEM).

Table 1 Main ingredients and formulations of the resin paste

Main ingredients	Content (%)
VE	100
Hydroquinone	0.04
TBPB	2.5
MgO	4.0
Zinc stearate	1.5

Atomic force microscope (AFM, Bruker Corporation, Germany) was used to characterize the surface roughness of carbon fibers. All AFM images were collected in air using the tapping mode with a silicon nitride probe with the scanning scope of 4 × 4 μm. Dynamic contact angle measurement was applied to characterize the wetting performance of different CFs by VE. Interfacial sheer strength (IFSS) of composites was tested by Interface Strength Tester (MODEL HM410, Japan). The polymer droplet was clamped by steel blades and pulled apart from fiber with a constant speed of 0.1 mm/min. More than 15 samples were tested. The IFSS (τ) between the CF and resin can be calculated using following formula: [25]

$$\tau = \frac{F_{\max}}{\pi d l} \tag{2}$$

where $F_{\max}$ is the maximum debonding force, d and l are diameter of the CFs and embedded length of CFs into matrix, respectively.

The tensile and flexural properties of the plain weave fabric reinforced composites were measured according to ASTM D3039 and ASTM D7264 standards, while the interlaminar shear strength of the unidirectional carbon fiber reinforced composites was measured based on ASTM D2344 standard. All tests were carried out on an Instron 5560 electronic universal mechanical testing machine at room temperature and 50% relative humidity. A minimum of five effective specimens of each sample were tested for statistical evaluation. The geometry of shear specimens was 15 × 5 × 2.5 mm^3, with a loading span length-to-specimen thickness ratio of 4.0. Dynamic mechanical analysis was performed using TA instrument DMA Q800 in flexural bending mode. Typical clamped sample dimensions were 30 × 13 × 3 mm^3. The oscillation amplitude of the instrument was 10 μm to insure that the viscoelastic response of the samples was linear. The temperature was ramped from 40 to 270 °C in 3 °C increments. The deformation frequency was 1 Hz. On completion of the measurements at 270 °C, the composite specimen was allowed to slow cool to room temperature in the instrument and the measurement procedure was repeated. All of the data used for this paper were taken from the second heat measurements in the DMA. This insures that each sample has the same thermal history. A minimum of three samples were measured for each group of composite specimens. The tensile properties of multifilament composites

were tested according to ASTM D4018-99 standard with a 150 mm gage length. A minimum of six effective specimens of each sample were tested for statistical evaluation. The density of carbon fibers was determined using Archimedes' method.

Results and discussion

Thermodynamics and kinetics of the grafting reaction

Table 2 shows the total electronic energies (E_{total}) of the three molecular at 0 K in Hartree and the finite temperature corrections for free energy ($G_{total}^{298.15K}$) arose from the various translational, rotational, and vibrational components at 298.15 K. The finite temperature-corrected value for free energy ($E_{Tcorr}^{298.15K}$) can be obtained simply by the addition of E_{total} and $G_{total}^{298.15K}$, which are shown in row 4 of the table. According to the formula (1), the $\Delta G_{reaction}^{298.15K}$ value for the reaction is −1.982 kcal/mol. The negative sign of the free energy indicates that this reaction will occur spontaneously at room temperature.

The reaction rate between AM and sizing agent was characterized by DSC. Figure 2a shows the heat and mass changes of the reaction at elevated temperature (5 °C/min). As can be seen from the mass curve, the weight of the sample dropped sharply in the initial stage because of the volatilization of solvent. A smaller endothermic peak near 45 °C was also observed on the heat curve corresponding to the weight loss. With the rise of temperature, the quality of the sample tended to be stable because all solvent was evaporated. AM began to react with sizing agent, and a strong exothermic peak appeared at 109 °C on the heat curve. After the peak, an obvious weight loss was observed again because of the volatilization of AM. It is apparent that AM can react with the sizing agent and the fastest reaction temperature is 109 °C at the heating rate of 5 °C/min. However, the modification temperature of CFs was set at 80 °C considering the water solubility and volatility of acrylamide. The DSC curves at constant temperature are shown in Fig. 2b. No significant weight loss was observed for the sample, and the reaction process was relatively mild. The reaction exothermic peak appeared at about 5 min. For a more complete reaction, the grafting time was set at 10 min.

FTIR spectrum of the product and epoxy sizing agent were characterized, as shown in Fig. 3. The peaks at 965 and 985 cm^{-1} represent the out-of-plane bending vibration of CH bond and the twisting vibration of $=CH_2$ in the olefin segments ($RCH=CH_2$), respectively. The particular absorption peaks at 1425 cm^{-1} (deformation vibration of CH_2) and 1675 cm^{-1} (stretching vibration of C=C) also arise from $RCH=CH_2$. Moreover, the peak at 1365 cm^{-1} corresponds to the stretching vibration of C–N bond in primary amide group ($–CO–NH_2$). The appearance or increase in these peaks after reaction is due to the addition of acrylamide (Fig. 3b). However, this is not enough to prove that acrylamide has reacted with the sizing agent. By comparison with the sizing agent spectrum, the intensity of epoxy group characteristic absorption peaks at 912, 829 and 1275 cm^{-1} decline significantly (Fig. 3b), which indicates that epoxy groups were involved in the reaction. In addition, the characteristic absorption peaks of secondary amide group (–CO–NH–) are observed after reaction at 3335 cm^{-1} (stretching vibration of NH), 1605, 1594 cm^{-1} (in-plane bending vibration of NH), 1620 cm^{-1} (stretching vibration of C=O) and 1230 cm^{-1} (shoulder peak, stretching vibration of C–N). Therefore, the essence of the grafting reaction is the reaction between amino group and epoxy group. This conclusion can be further proved by the enhancement of peaks at 3200 cm^{-1} (stretching vibration of OH) and 619 cm^{-1} (out-of-plane bending vibration of COH), which arise from the formation of alcoholic hydroxyl group, as shown in Fig. 1.

Surface morphology and surface roughness of carbon fiber

SEM images for CFs, DCFs and MCFs are shown in Fig. 4. As shown in Fig. 4a, e, both CFs and DCFs surface are smooth before grafting modification.

Table 2 Calculation results of thermodynamics for the reaction between epoxy sizing agent and AM

	Epoxy sizing agent	AM	Product
E_{total} (Hartree)	−1501.7742219	−247.3241822	−1749.1281205
$G_{total}^{298.15K}$ (kcal/mol)	317.923	30.174	364.763
$E_{Tcorr}^{298.15K}$ (Hartree)	−1501.2675798	−247.2760969	−1748.5468341

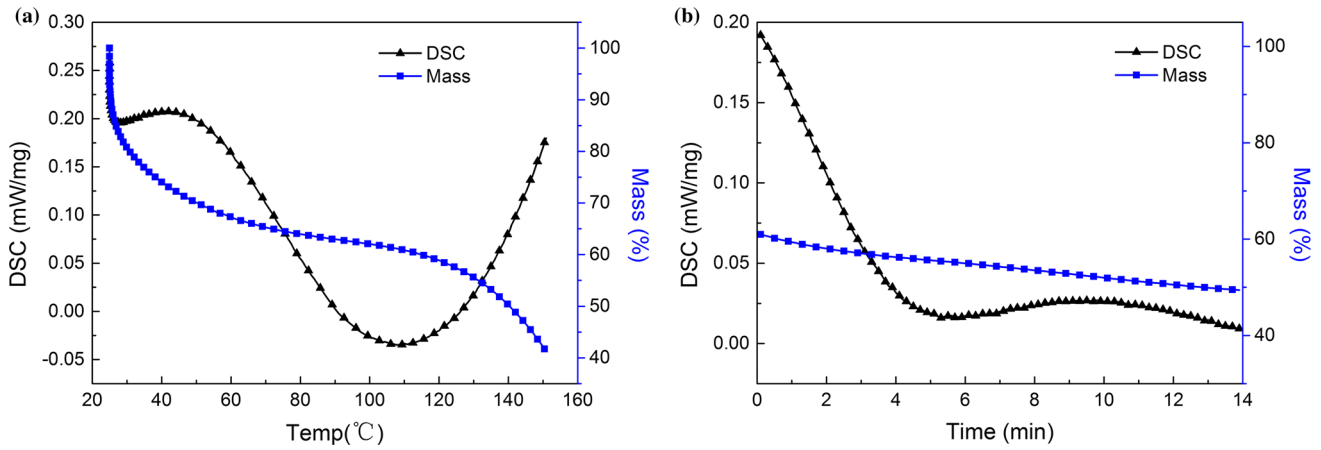

Figure 2 DSC curves of the reaction between acrylamide and sizing agent **a** at elevated temperature (5 °C/min), **b** at constant temperature (80 °C).

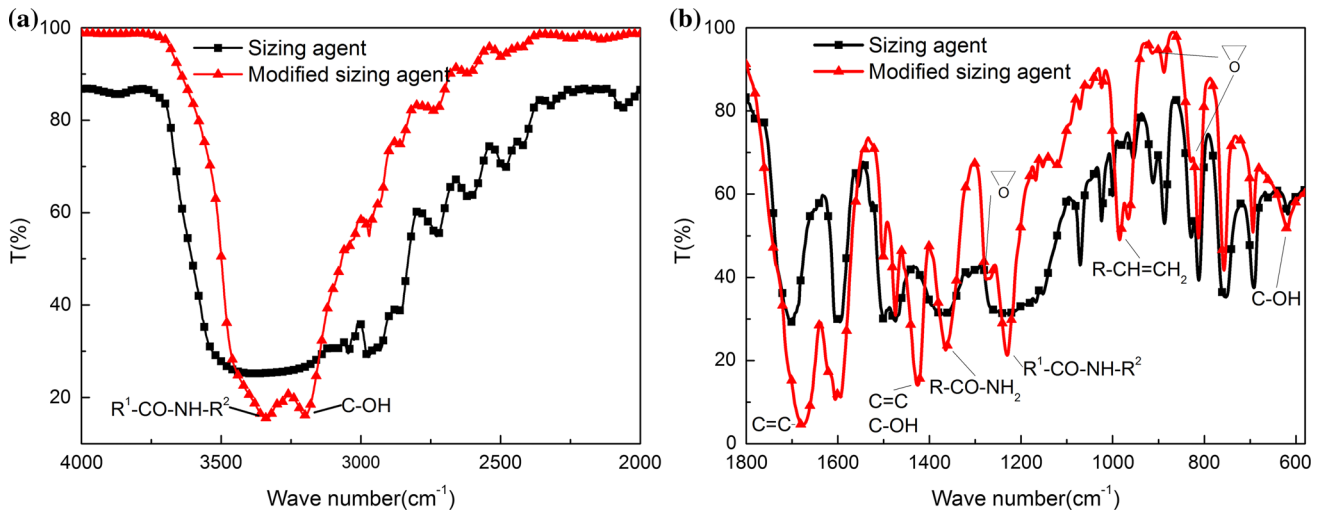

Figure 3 FT-IR spectra of the sizing agent before and after modification. **a** high frequency region, **b** low frequency region.

After treated by acrylamide aqueous solution with different concentrations, two carbon fibers exhibited different surface morphologies. When the concentration was 0.5 or 1.0%, the surface grafting process had no remarkable influence on the morphology of both carbon fibers (Fig. 4b, c, f, g). However, significant difference was observed when the concentration was increased to 1.5%. As shown in Fig. 4d, h, a mass of acrylamide crystals gathered on the surface of CFs while DCFs still exhibited a smooth surface with few acrylamide crystals. This result indicates that the sizing agent on CFs surface is attractive to acrylamide molecules. Thus, acrylamide molecules could migrate from the modifier solution to CFs surface and react with the sizing agent easily. Because of the imperfection in the preparation process, DCFs surface also contains a small amount of polar functional groups, such as carboxyl and epoxy groups [26, 27]. These polar functional groups can also react with AM, which resulted in the slight enrichment of acrylamides in DCFs surface. The unstable acrylamide crystals in CFs surface are unhelpful to the interface performance of composites. Therefore, 1.0% may be the best concentration of AM solution.

Figure 5 shows the surface topography of different carbon fibers tested by atomic force microscope (AFM). The roughness data calculated from AFM images are listed in Table 3. It can be learned from the images that the grafting modification by AM had no obvious effect on the surface topography of carbon fibers. The surface roughness of MCF and MDCF were also increased slightly. As expected, the growth

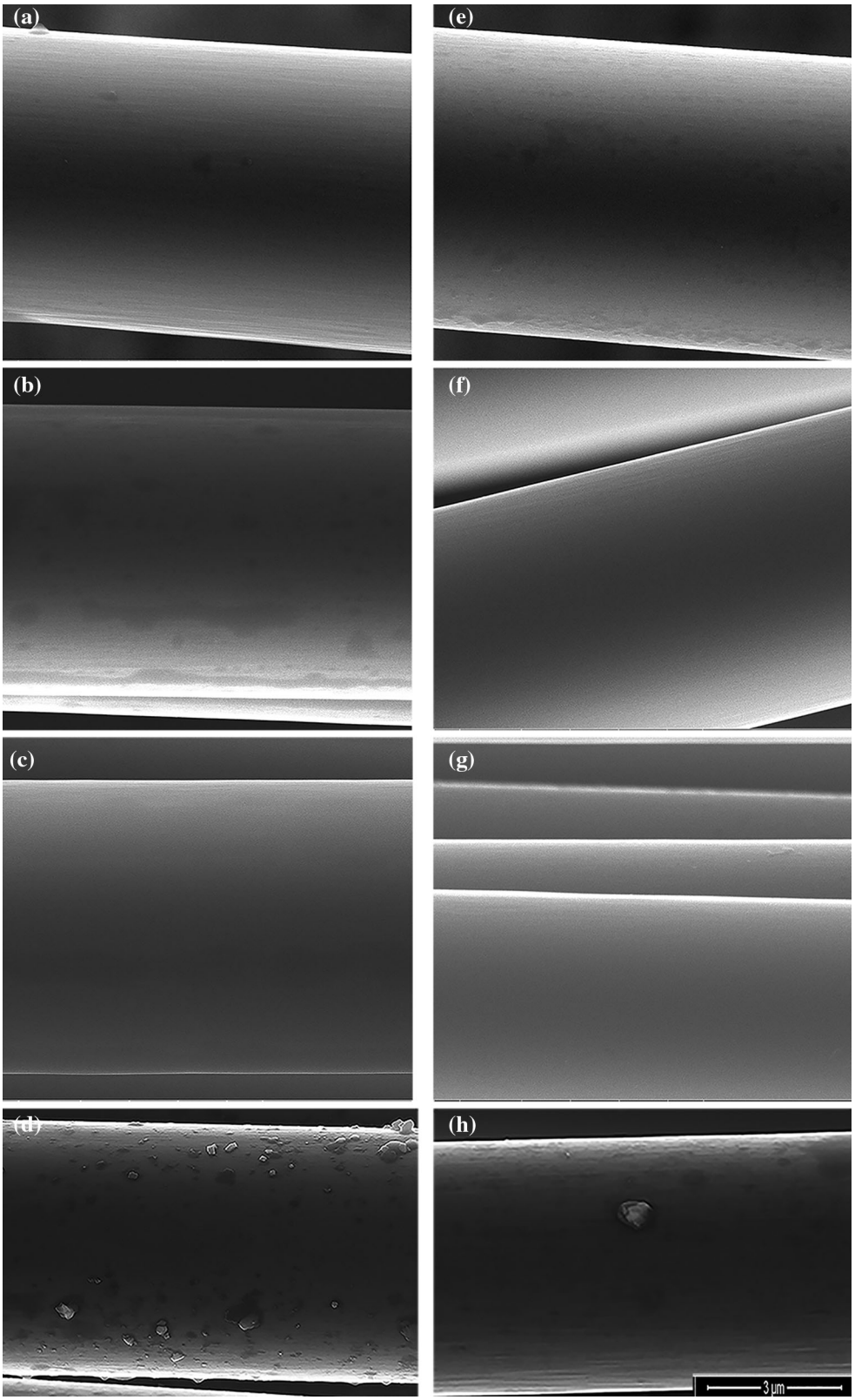

Figure 4 SEM images for **a** CF, MCF grafted, **b** by 0.5%AM, **c** by 1.0%AM, **d** by 1.5%AM, **e** DCF, MDCF grafted, **f** by 0.5%AM, **g** by 1.0%AM and **h** by 1.5%AM, ×30,000.

range for MCF (7.98%) was higher than MDCF (3.73%). MCF exhibited the roughest surface with 176 nm. The increase in surface roughness can improve the interfacial adhesion of composites by increasing fiber surface area and enhancing mechanical interlocking between the fiber and matrix.

Table 3 Surface roughness of the different carbon fibers calculated from the AFM images

	CF	DCF	MCF	MDCF
R_a (nm)	163	134	176	139
Standard deviation (nm)	36.7	27.5	43.2	34.8

Surface composition of carbon fiber

Raman spectroscopy can be well utilized to identify the molecular structure and characterize the order/disorder structure of carbon materials. Figure 6 presents the Raman spectra of AM and different carbon fibers. Two main characteristic Raman responses were observed in the Raman spectra of carbon fibers in accordance with reports done by other researchers [28, 29]. The D-band at around 1340 cm^{-1} is related to the breathing mode of the sixfold aromatic ring near the graphite basal edge, while the G-band at around 1590 cm^{-1} is assigned to the in-plane bond stretching mode of hybridized sp^2 C atoms [30]. For CFs (Fig. 6a), the intensities of both D-band and G-band decreased simultaneously with the grafting of acrylamide, probably due to the inhibition of incident laser caused by AM on fiber surface. This phenomenon was not found on the Raman spectra of DCFs (Fig. 6b), which indicates that acrylamide is more likely to react with epoxy sizing agent on CFs surface. In addition to the two main peaks, some new characteristic bands were observed in the Raman spectra, located at around 1850 and 790 cm^{-1} according to the peak fitting analysis (Fig. S3 and Table S1). The intensities of the new characteristic bands for CFs (Fig. 6a) were greater than that for DCFs (Fig. 6b), which indicates that these new bands were caused by the introduction of AM on CFs surface. When the concentration of AM aqueous solution was 1.0 wt%, the intensities of D-band and G-band decreased most and the new bands raised most, which is consistent with the results of SEM and AFM.

XPS survey scans were performed to detect the surface elements of the carbon fibers surface. The

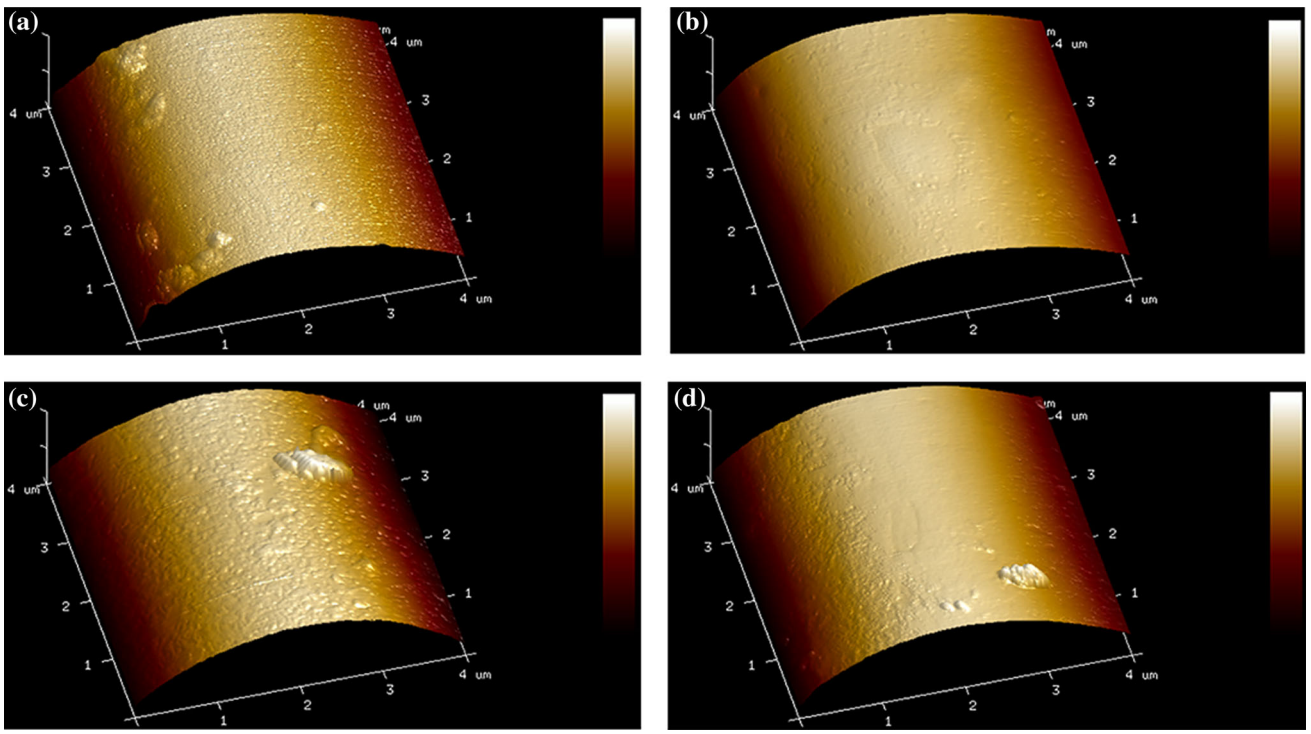

Figure 5 AFM images for **a** CF, **b** DCF, **c** MCF grafted by 1.0%AM and **d** MDCF grafted by 1.0%AM.

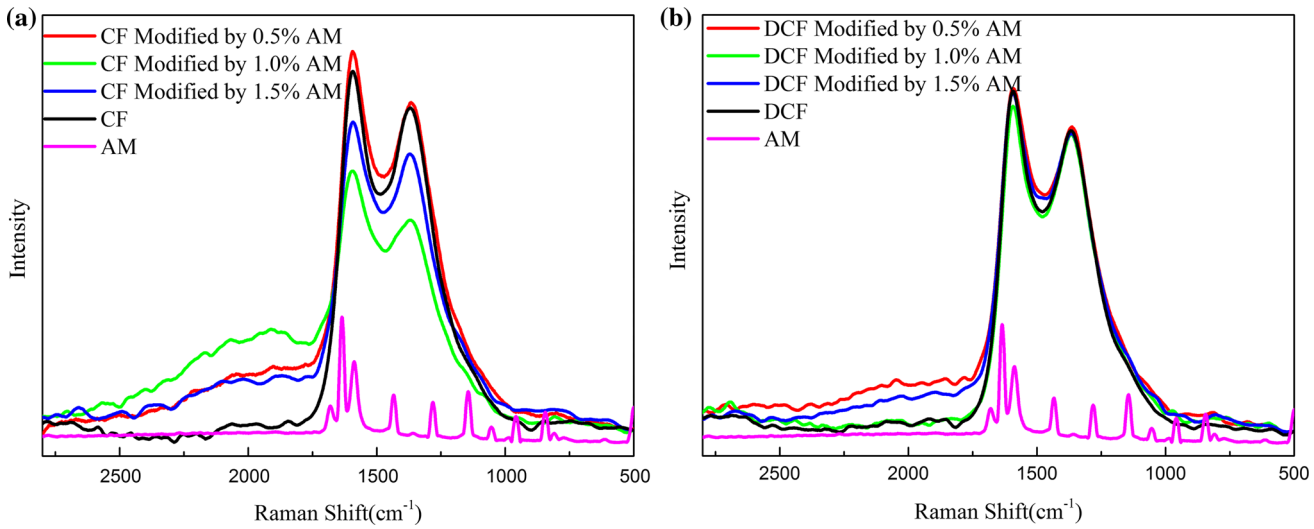

Figure 6 Raman spectra of **a** CF and **b** DCF modified by AM with different concentrations.

wide survey spectra of carbon fibers are shown in Fig. 7a–d. Both CFs and DCFs surface are composed mainly of carbon, oxygen and a small amount of nitrogen. After the modification, the contents of nitrogen on the surface of CFs and DCFs were increased by 0.64 and 0.31%, respectively. This increase in N1*s* peak intensity was identified to the amide functional groups of AM which migrated and grafted onto the surface of CFs and DCFs. It is obvious that AM is more likely to react with CFs than DCFs.

A detailed analysis of the XPS spectra was carried out by peak fitting of C1*s* peaks and N1*s* peaks. Deconvolution of the C1*s* peak of CFs and DCFs before and after grafting are shown in Fig. 7e–h. The positions used for the peak fitting are detailed in Table 4 [31], together with the atomic concentrations calculated from the quantification of the individual components. The fitted peak at around 284.60 eV is assigned to the graphite regular carbon and the peak at 285.45 eV is corresponded to the amorphous carbon on carbon fiber surface. After grafting, the concentration of regular carbon was decreased while the amorphous carbon was increased for both carbon fibers. In addition to the concentration, the full width at half maximum (FWHM) of the peak at 284.60 eV was also increased by AM molecules (from 1.480 to 1.724 for CFs and 1.272 to 1.409 for DCFs). These results together with the enhancement of –(C=O)– peak at 287.80 eV manifest the successful grafting of AM on the two carbon fibers. Furthermore, the reaction mechanisms of AM with the two carbon fibers were proved by the changes of C1*s* peaks. As shown in Table 4, the concentration of –C–OR peak for MCF was decreased, which indicates that AM was grafted on CFs surface by reacting with the epoxy groups of the sizing agent (Fig. 8a). The disappearance of –COOR peak for MDCF indicates that AM reacted with carboxyl functional groups on DCFs surface (Fig. 8b). Figure 7i, j show the deconvolution of the N1*s* peak of MCFs and MDCFs. Table 5 details the main positions used for the peak fitting and the atomic concentrations. The concentration of O=C–N peak at around 400.76 eV for MDCFs was significantly greater than that for MCFs, which resulted from the reaction between AM and carboxyl functional group, as shown in Fig. 8b.

Wettability and interfacial shear strength

The interfacial compatibility between fibers and vinyl ester resin was characterized by dynamic contact angle measurement. The specific measurement method was described by Zhang [8], and the results are shown in Table 6. It can be learn from the results that grafting of AM had no significant effect on the contact angle with VE for both carbon fibers. Due to the structural similarity with epoxy sizing agent, VE can wet pristine CFs easily (76.37°). Grafting of AM with the sizing agent only had a slight impact on the carbon fiber surface morphology. Therefore, the wettability of MCFs has not been promoted visibly (75.20°). Without sizing agent, the wettability of DCFs was poor (92.45°) because of the highly stable,

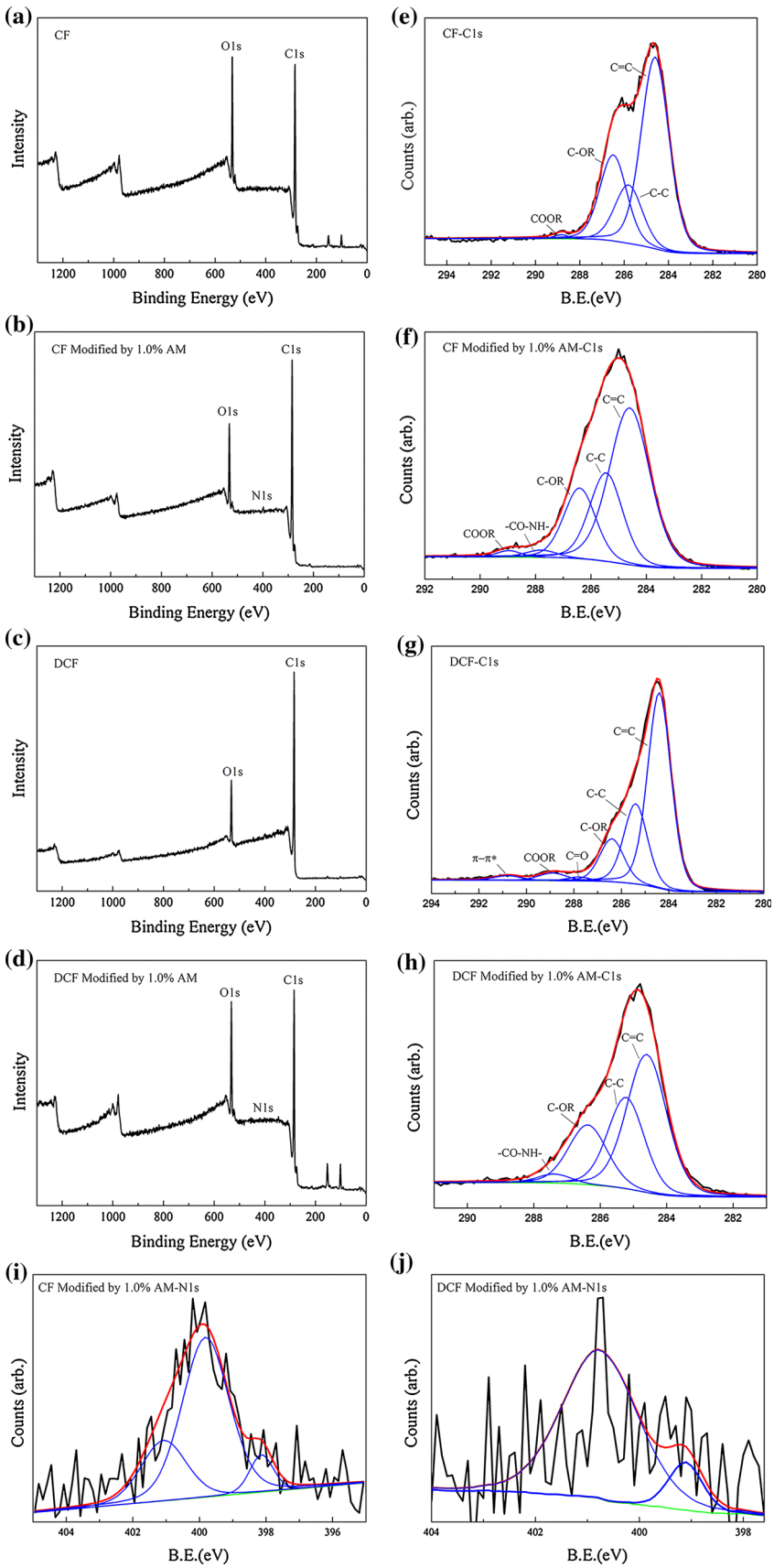

Figure 7 XPS wide survey spectrums of the **a** CF, **b** CF modified by 1.0% AM, **c** DCF and **d** DCF modified by 1.0% AM. High-resolution C1*s* XPS scans of **e** CF, **f** CF modified by 1.0% AM, **g** DCF, **h** DCF modified by 1.0% AM. High-resolution N1*s* XPS scans of **i** CF modified by 1.0% AM and **j** DCF modified by 1.0% AM.

Table 4 XPS C1*s* peak fitting results for CF and DCF before and after modified by AM

Type	C=C		C–C		C–OR		C=O		COOR	
	B.E. (eV)	P.C. (%)	B.E. (eV)	P.C. (%)	B.E. (eV)	P.C. (%)	B.E. (eV)	P.C. (%)	B.E. (eV)	P.C. (%)
CF	284.60	57.45	285.80	17.26	286.49	24.72	–	–	288.84	0.57
MCF	284.60	53.54	285.45	25.49	286.40	18.89	287.80	1.82	288.96	0.26
DCF	284.50	61.97	285.70	16.56	286.40	15.73	287.80	1.61	288.90	1.72
MDCF	284.60	48.04	285.22	29.21	286.37	20.11	287.38	2.64	–	–

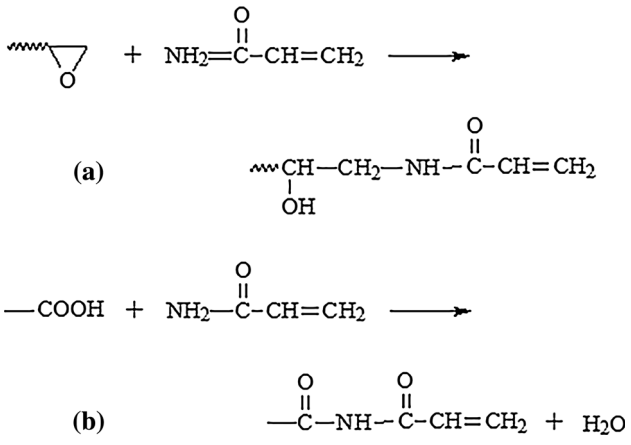

Figure 8 Mechanisms of AM react with **a** CF and **b** DCF.

nonpolar and smooth graphitic surface. The slight improvement of wettability (89.30°) for MDCFs was attributed to the grafting of AM on DCFs surface.

Micro-droplet tests (Fig. 9a) were performed to investigate the interface shear strength (IFSS) between VE matrix and carbon fibers. Test results are shown in Fig. 9, together with the SEM micrographs after debonding. A significant increase in IFSS can be observed for MCFs reinforced micro-droplet composite (58.26 ± 2.21 MPa) compared with CFs reinforced micro-droplet composite (31.67 ± 1.51 MPa). This improvement of IFSS (86.96%) was benefitted to a large extent from the vinyl functionalization of CFs surface by the grafting of AM. Covalent bonds were formed between MCFs and VE matrix, and more residual matrix was observed on MCFs surface (Fig. 9d) after debonding. Compared with DCFs reinforced micro-droplet composite (24.39 ± 1.62 MPa), the IFSS of MCFs was increased by 138.87%, higher than that described in the literature [17], which is probably due to the toughening effect of the sizing agent at the interface. Different with CFs, surface grafting of AM on DCFs surface had no significant

Table 5 XPS N1*s* peak fitting results for CF and DCF after modified by AM

Type	C–N		O=C–N	
	B.E. (eV)	P.C. (%)	B.E. (eV)	P.C. (%)
MCF	399.82	67.52	401.08	24.59
MDCF	399.11	12.61	400.76	87.39

Table 6 Results of contact angle between different fibers and VE

Carbon fibers	CF	MCF	DCF	MDCF
Contact angle (°)	76.37	75.20	92.45	89.30

effect on IFSS (Fig. 9b) and SEM micrograph after debonding (Fig. 9e, f). Few chemical bonds were formed between MDCFs and VE matrix because of the lower carboxyl group content on DCFs surface. Acid oxidation process as described in the literature [17] can significantly increase the carboxyl group content on fiber surface at the expense of the strength of carbon fiber, which will be discussed below.

Interlaminar shear strength of composites

Interlaminar shear tests of unidirectional composites were performed to verify the effect of the graft modification [25]. As can be seen from the histogram in Fig. 10, the interlaminar shear strength of MCFs/VE composite (77.37 ± 2.13 MPa) was increased by 55.61% than CFs/VE composite (49.72 ± 1.56 MPa), which can be explained by the same reason as the increase in IFSS. The covalent bonds in interface phase promoted the load transfer from matrix to carbon fibers and enhanced the interlaminar shear [32, 33]. The SEM images of interlaminar shear fracture surfaces of CFs/VE and MCFs/VE composites are shown in Fig. 11. It was obvious that more

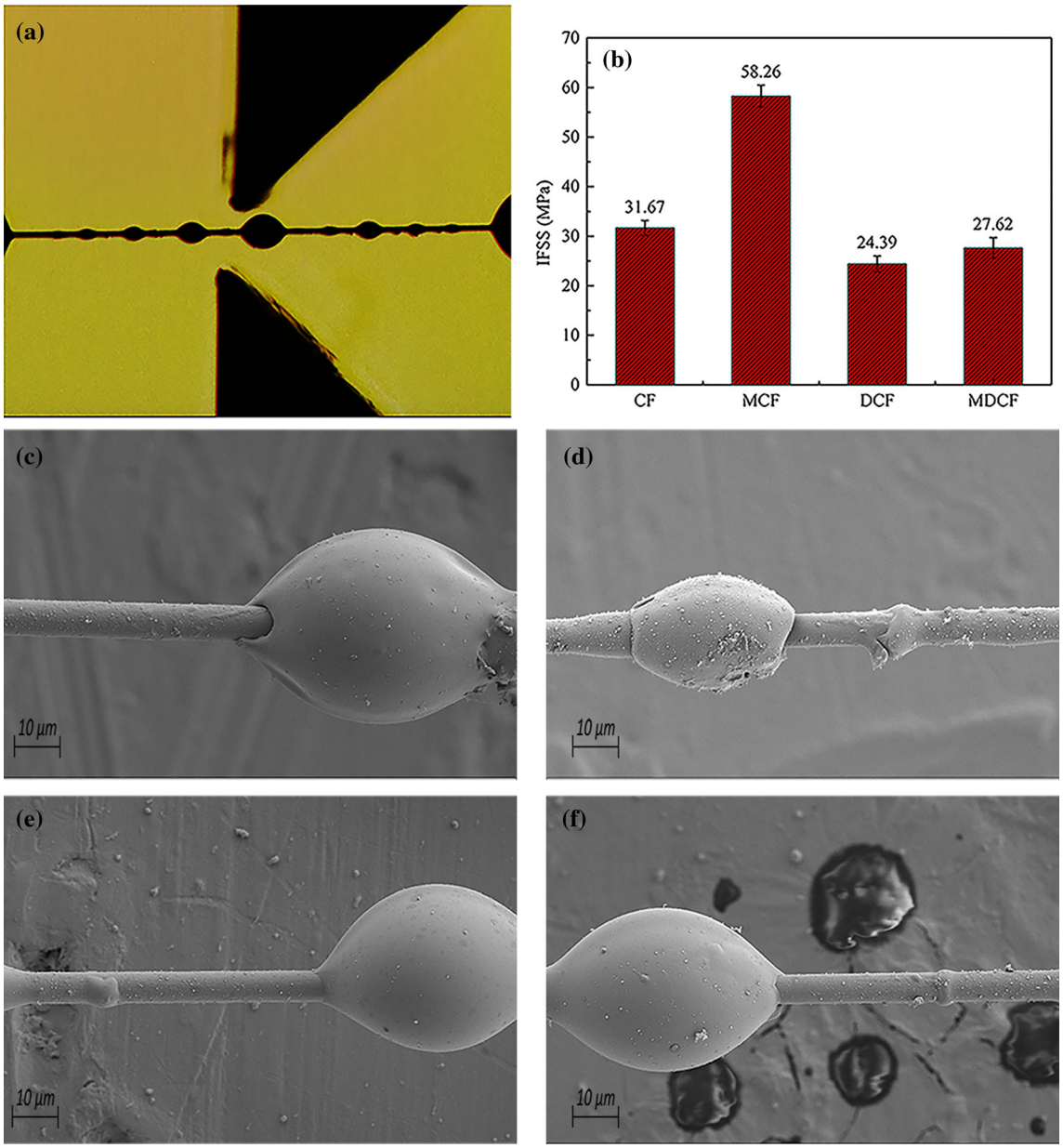

Figure 9 Image of micro-droplet test for the interfacial shear strength between VE matrix and CF (**a**). IFSS results for different carbon fibers with VE (**b**). Debonded interfaces for **c** CF, **d** MCF, **e** DCF and **f** MDCF.

residual resin matrix was observed on MCFs surface after interlaminar shear tests. This was consistent with the result of micro-droplet tests. In addition, the destructive modes of the two composites were distinguished clearly by the SEM images. For CFs/VE composites, resin matrix was debonded in interphase, leaving a smooth CFs surface without residual resin matrix, as shown in Fig. 11b. However, the cracks at the interface of MCFs/VE composites were deflected into resin matrix due to the strong interfacial bonding, as shown in the square frame in Fig. 11d. Therefore, a large amount of residual resin was observed on the surface of MCFs after interlaminar shear tests and the interlaminar shear strength was improved significantly.

Dynamic mechanical analysis

Dynamic mechanical analysis of composite materials has been used extensively to draw conclusions pertaining to the level of interaction between the matrix polymer and fiber reinforcement. The viscoelastic

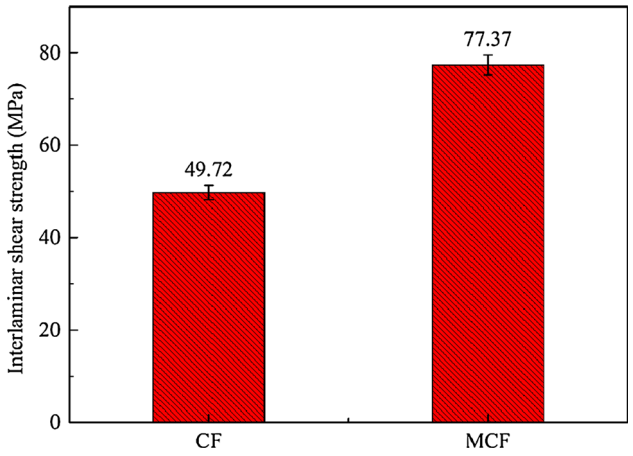

Figure 10 Interlaminar shear strength of the composites prepared with different carbon fibers.

response (storage modulus E' and damping ratio tan δ) obtained at 1 Hz for the composite samples are illustrated in Fig. 12. From the E' curves, it can be seen that the glassy modulus was elevated from approximately 8921 MPa for the CFs/VE composite to about 10445 MPa for the MCFs/VE composite. The rubbery modulus was also enhanced by the surface modification of CFs. The glass-to-rubber transition region of the modified composite sample was also broader than the pristine composite. A closer examination of the glass-to-rubber transition of the two composites can be seen in the tan δ curves (1 Hz) shown in Figs. 12b. The tan δ curve for MCFs/VE composite was much broader than CFs/VE composite. And the temperature for glass-to-rubber transition (T_g) was elevated by 13.24 °C from 160.38 °C for CFs/VE composite to 173.62 °C for MCFs/VE composite. This increased E', T_g and peak broadness of tan δ could be all due to the formation of new covalent bonds between carbon fiber and VE. An elevated degree of chemical interaction between the fiber and resin matrix could improve the effectiveness of load transfer by the interphase and restrict the mobility of the polymer chains in the interphase region.

The mechanical properties of composites

The mechanical properties of composites are influenced largely by the interface phase between CFs and resin matrix [25]. Figure 13 presented the tensile and flexural properties of composites reinforced by CFs and MCFs. As shown in Fig. 13a, the MCFs reinforced composites showed higher tensile strength (924.79 ± 68.42 MPa) and Young's modulus (57.78 ± 6.53 GPa). The increments were 35.52% for tensile strength and 30.34% for Young's modulus. This remarkable increase in the tensile strength and Young's modulus may be due to the covalent bonds

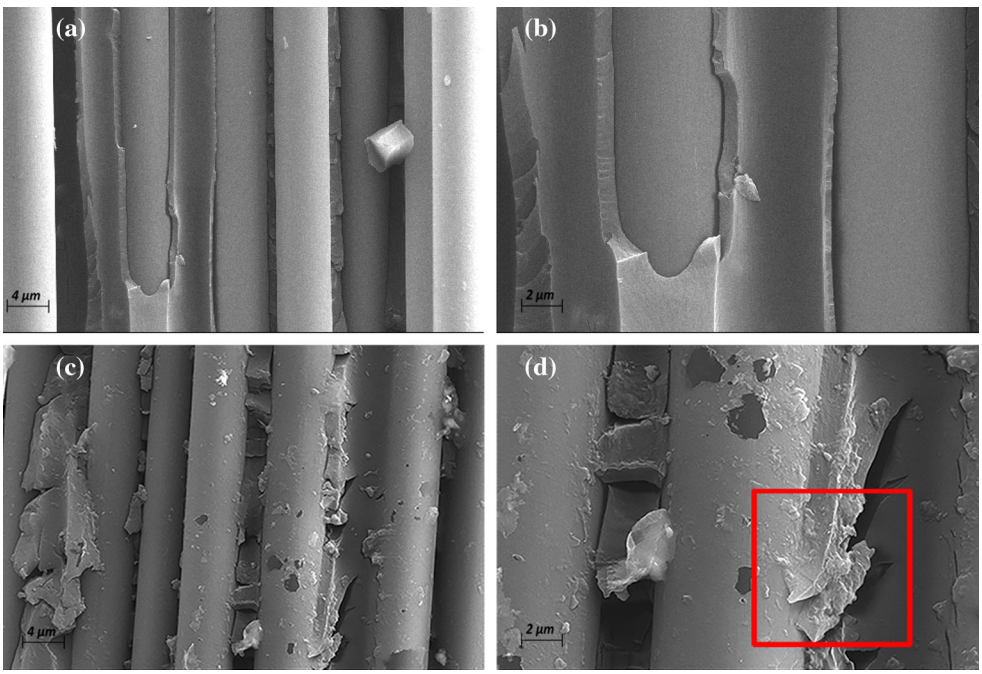

Figure 11 SEM images of interlaminar shear fracture surfaces of CF/VE composites **a**, **b** CF/VE, **c**, **d** MCF/VE. The *square frame* in (**d**) shows the deflection of crack into VE matrix.

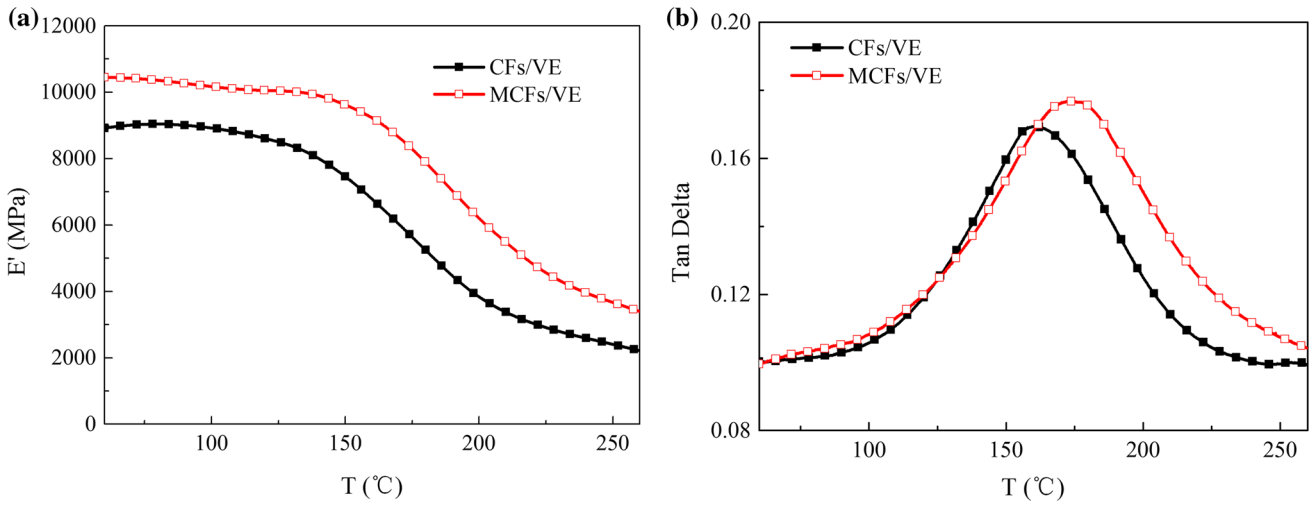

Figure 12 Storage modulus (**a**) and damping ratio (**b**) curves for composite samples versus temperature obtained from DMA (1 Hz).

between MCFs surface and resin matrix formed during the curing of VE by free-radical polymerization. The load applied to the resin matrix was more efficiently transferred to the carbon fibers and the composites exhibited more excellent tensile properties. It can be seen from the error bars that the dispersion of tensile properties was increased due to the nonuniform graft modification. A continuous process may reduce this discretization.

Flexural properties of the composites were more affected by the interfacial bonding properties. The representative flexural properties are shown in Fig. 13b. After surface grafting modification of carbon fibers, the flexural strength was increased by 40.34%, from 509.47 ± 66.24 MPa for CFs/VE composites to 714.99 ± 86.50 MPa for MCFs/VE composites, and the flexural modulus was enhanced by 35.84% to 43.21 ± 3.42 GPa. These increased flexural properties could be explained by the same reason as the increase in tensile properties. That is the covalent bonds in the interface phase introduced by the grafting of AM on carbon fibers surface. To obtain valid flexural strength, the standard support span-to-thickness ratio (32:1) was chosen. The failure mode of two kinds of composites were compression on the outer surfaces of the specimens at loading nose, without a interlaminar shear failure or a crushing failure under a support or loading nose. A better interface connection allowed the load on the outer surface to be transferred to the internal fibers efficiently. Therefore, MCFs/VE composites exhibited higher flexural performance.

The increments of tensile and flexural properties were both smaller than that of IFSS because that the

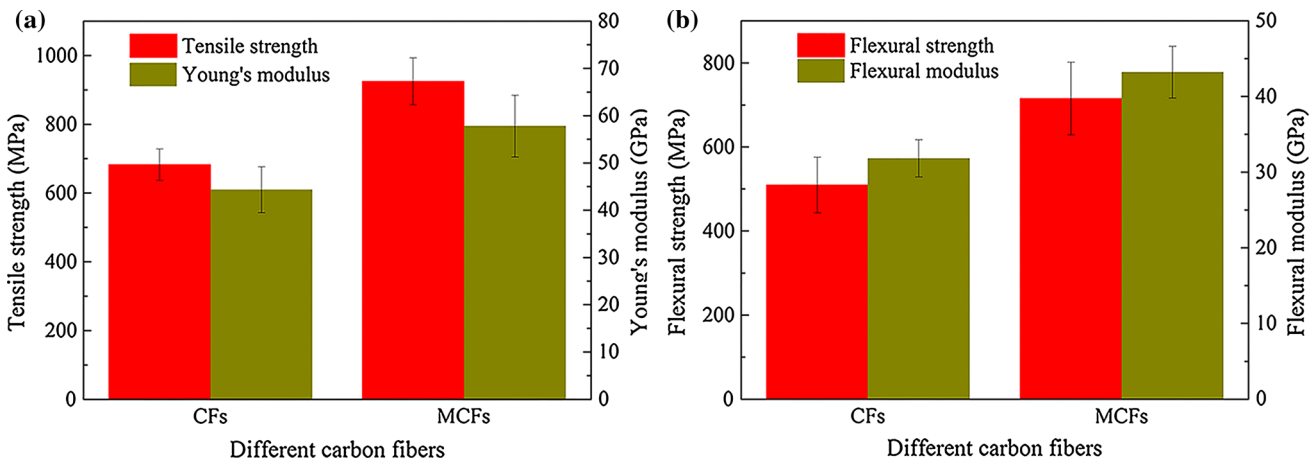

Figure 13 Tensile properties (**a**) and flexural properties (**b**) of CFs and MCFs reinforced composites.

mechanical properties are more dominated by the fiber and resin matrix and there are more defects and gaps for laminated composites than micro-droplet composites for IFSS tests. However, the increments of mechanical properties in this study are greater significantly than the values described in the literature [17]. There may be several reasons. First, although vinyl functionalization on oxidized carbon fiber surface could covalently bond carbon fibers and VE, the interface between the two phases is rigid, which is detrimental to the interface performance. The disparity of the increase between macroscopic mechanical strength (19.4%) and interfacial shear strength (90.53%) for APMA-CF/VE composites has proved it. In this study, vinyl functionalization was carried out on the sizing agent of CFs. The sizing agent could swell into VE before curing process to reduce the interfacial stress caused by cure volume shrinkage of VE [18]. A strong and tough interface was formed for the composite. In addition, sizing process plays an important role in protecting carbon fibers from fracture and fluffiness. In the literature [17], CFs was desized and further oxidized by H_2SO_4/HNO_3 mixture, which may introduce defects on carbon fibers surface and cause decrease in carbon fiber strength [34]. Multifilament composites were used to measure the strength of carbon fibers treated by different methods. The results are shown in Fig. 14. It can be seen from the histogram that the strength of carbon fibers decreased in varying degrees for DCFs and OCFs as predicted. This is another shortcoming for the vinyl functionalization on oxidized carbon fibers surface. For MCFs prepared in this study, no significant decline in strength was observed, which explains the significant enhancement in IFSS, dynamic and static mechanical properties of MCFs/VE composites.

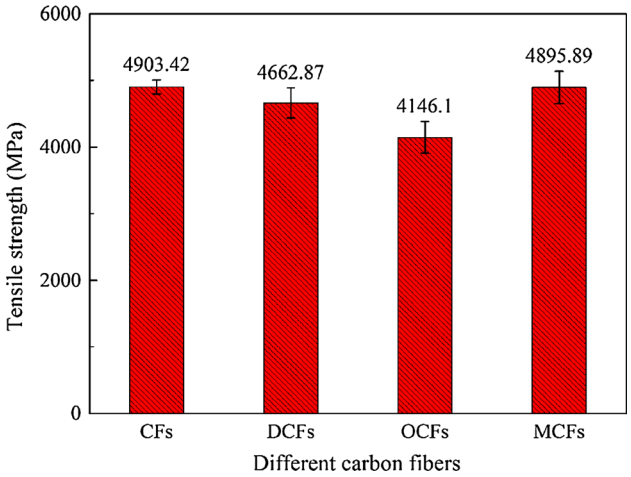

Figure 14 Strength of multifilament composites reinforced by different carbon fibers.

Conclusion

In this paper, the epoxy sizing agent on carbon fibers (CFs) surface was functionalized by acrylamide (AM) to improve the interfacial bonding with vinyl ester resin (VE). The reaction between AM and epoxy sizing agent is feasible, and the optimum reaction condition is 10 min at 80 °C on the base of the thermodynamics calculation and kinetics study. Under this condition, CFs surface was grafted by AM in aqueous solution to obtain modified carbon fibers (MCFs). The surface morphology (SEM), surface roughness (AFM) and surface composition (Raman spectra and XPS) of MCF indicated that AM was grafted onto CFs surface successfully by reacting with the epoxy groups of the sizing agent. The optimal concentration of AM aqueous solution is 1.0 wt%. No significant improvement of wettability with VE was observed for MCFs. However, MCFs/VE composites exhibited 86.96 and 55.61% elevation in interface shear strength and interlaminar shear strength compared with pristine CFs/VE composites, which were benefited from the covalent bonds between carbon fibers and VE matrix and the interface toughness due to the swelling effect of the sizing agent. Covalent bonds in interphase promote the load transfer from matrix to carbon fibers, and the sizing agent could reduce the internal stress and avoid brittle fracture at the interface. It is due to the strong and tough interface that cracks in the interface region of MCFs/VE composites were deflected into resin matrix and more resin matrix remained on the surface of carbon fibers. In addition, the protection of sizing agent to carbon fibers may be another reason for the significant improvement of dynamic and static mechanical properties for MCFs/VE composites. After grafted by AM, the glassy modulus was enhanced by 17.08% and the temperature for glass-to-rubber transition (T_g) was elevated by 13.24 °C. The increments for tensile strength and flexural strength were 35.52 and 40.34%, respectively.

Acknowledgements

The authors acknowledge the support of the High Performance Computing Center of the Harbin Institute of Technology. This research did not receive any specific grant from funding agencies in the public, commercial, or not-for-profit sectors.

Electronic supplementary material: The online version of this article (doi:10.1007/s10853-017-1485-8) contains supplementary material, which is available to authorized users.

References

[1] Liu W, Jiao W, Yang F, Wang R, Li L, Jiao W (2016) Study on rheological behavior of vinyl ester resin during thickening. J Vinyl Addit Technol. doi:10.1002/vnl.21572

[2] Gnaedinger F, Middendorf P, Fox B (2016) Interfacial shear strength studies of experimental carbon fibres, novel thermosetting polyurethane and epoxy matrices and bespoke sizing agents. Compos Sci Technol 133:104–110

[3] Liu Z, Hao B, Zhang Y (2015) Control interfacial properties and tensile strength of glass fibre/PP composites by grafting poly(ethylene glycol) chains on glass fibre surface. RSC Adv 5:40668–40677

[4] Wang Y, Hahn TH (2007) AFM characterization of the interfacial properties of carbon fiber reinforced polymer composites subjected to hygrothermal treatments. Compos Sci Technol 67:92–101

[5] Zhang X, Fan X, Yan C, Li H, Zhu Y, Li X, Yu L (2012) Interfacial microstructure and properties of carbon fiber composites modified with graphene oxide. ACS Appl Mater Interface 4:1543–1552

[6] Li Y, Li Y, Ding Y, Peng Q, Wang C, Wang R, Sritharan T, He X, Du S (2013) Tuning the interfacial property of hierarchical composites by changing the grafting density of carbon nanotube using 1,3-propodiamine. Compos Sci Technol 85:36–42

[7] Rong H, Dahmen K, Garmestani H, Yu M, Jacob KI (2013) Comparison of chemical vapor deposition and chemical grafting for improving the mechanical properties of carbon fiber/epoxy composites with multi-wall carbon nanotubes. J Mater Sci 48:4834–4842. doi:10.1007/s10853-012-7119-2

[8] Zhang S, Liu WB, Hao LF, Jiao WC, Yang F, Wang RG (2013) Preparation of carbon nanotube/carbon fiber hybrid fiber by combining electrophoretic deposition and sizing process for enhancing interfacial strength in carbon fiber composites. Compos Sci Technol 88:120–125

[9] Xu H, Zhang X, Liu D, Chun Y, Fan X (2014) A high efficient method for introducing reactive amines onto carbon fiber surfaces using hexachlorocyclophosphazene as a new coupling agent. Appl Surf Sci 320:43–51

[10] Yu J, Meng L, Fan D, Zhang C, Yu F, Huang Y (2014) The oxidation of carbon fibers through $K_2S_2O_8/AgNO_3$ system that preserves fiber tensile strength. Compos B Eng 60:261–267

[11] Cao HL, Huang YD, Zhang ZQ, Sun JT (2005) Uniform modification of carbon fibers surface in 3-D fabrics using intermittent electrochemical treatment. Compos Sci Technol 65:1655–1662

[12] Zhao F, Huang Y (2011) Uniform modification of carbon fibers in high density fabric by gamma-ray irradiation grafting. Mater Lett 65:3351–3353

[13] Li J, Huang Y, Fu S, Yang L, Qu H, Wu G (2010) Study on the surface performance of carbon fibres irradiated by gamma-ray under different irradiation dose. Appl Surf Sci 256:2000–2004

[14] Dilsiz N, Wightman JP (1999) Surface analysis of unsized and sized carbon fibers. Carbon 37:1105–1114

[15] Sawada Y, Nakanishi Y, Fukuda T (1993) effect of carbon-fiber surface on interfacial adhesive strengths in CFRP. Composites 24:573–579

[16] Qian X, Wang X, OuYang Q, Chen Y, Yan Q (2012) Surface structural evolvement in electrochemical oxidation and sizing and its effect on carbon fiber/epoxy composites properties. J Reinf Plast Compos 31:999–1008

[17] Zhang X, Liu L, Li M, Chang Y, Shang L, Dong J, Xiao L, Ao Y (2016) Improving the interfacial properties of carbon fibers/vinyl ester composites by vinyl functionalization on the carbon fiber surface. RSC Adv 6:29428–29436

[18] Xu L (2003) Interfacial engineering of the interphase between carbon fibers and vinyl ester resin. Michigan State University, East Lansing

[19] Broyles NS, Verghese K, Davis RM, Lesko JJ, Riffle JS (2005) Pultruded carbon fiber vinyl ester composites processed with different fiber sizing agents. Part I: processing and static mechanical performance. J Mater Civ Eng 17:320–333

[20] Robertson M, Bump MB, Verghese KE, McCartney SR, Lesko JJ, Riffle JS, Kim IC, Yoon TH (1999) Designed interphase regions in carbon fiber reinforced vinyl ester matrix composites. J Adhes 71:395–416

[21] Broyles NS, Verghese K, Davis SV, Li H, Davis RM, Lesko JJ, Riffle JS (1998) Fatigue performance of carbon fibre vinyl ester composites: the effect of two dissimilar polymeric sizing agents. Polymer 39:3417–3424

[22] Verghese K, Jensen RE, Lesko JJ, Ward TC (2001) Effects of molecular relaxation behavior on sized carbon fiber-vinyl ester matrix composite properties. Polymer 42:1633–1645

[23] Sun H (1998) COMPASS: an ab initio force-field optimized for condensed-phase applications—overview with details on alkane and benzene compounds. J Phys Chem B 102:7338–7364

[24] Jiao W (2014) Preparation and characterization of chopped carbon fiber reinforced vinyl ester resin sheet molding compound. Harbin Institute of Technology, Harbin

[25] Wang C, Li Y, Tong L, Song Q, Li K, Li J, Peng Q, He X, Wang R, Jiao W, Du S (2014) The role of grafting force and surface wettability in interfacial enhancement of carbon nanotube/carbon fiber hierarchical composites. Carbon 69:239–246

[26] Jang C, Nouranian S, Lacy TE, Gwaltney SR, Toghiani H, Pittman CU Jr (2012) Molecular dynamics simulations of oxidized vapor-grown carbon nanofiber surface interactions with vinyl ester resin monomers. Carbon 50:748–760

[27] Nouranian S, Jang C, Lacy TE, Gwaltney SR, Toghiani H, Pittman CU Jr (2011) Molecular dynamics simulations of vinyl ester resin monomer interactions with a pristine vapor-grown carbon nanofiber and their implications for composite interphase formation. Carbon 49:3219–3232

[28] Jin SY, Young RJ, Eichhorn SJ (2014) Controlling and mapping interfacial stress transfer in fragmented hybrid carbon fibre-carbon nanotube composites. Compos Sci Technol 100:121–127

[29] Li Z, Young RJ, Wang R, Yang F, Hao L, Jiao W, Liu W (2013) The role of functional groups on graphene oxide in epoxy nanocomposites. Polymer 54:5821–5829

[30] Ferrari AC, Robertson J (2000) Interpretation of Raman spectra of disordered and amorphous carbon. Phys Rev B 61:14095–14107

[31] An Q, Rider AN, Thostenson ET (2012) Electrophoretic deposition of carbon nanotubes onto carbon-fiber fabric for production of carbon/epoxy composites with improved mechanical properties. Carbon 50:4130–4143

[32] Liao W, Tien H, Hsiao S, Li S, Wang Y, Huang Y, Yang S, Ma CM, Wut Y (2013) Effects of multiwalled carbon nanotubes functionalization on the morphology and mechanical and thermal properties of carbon fiber/vinyl ester composites. ACS Appl Mater Interface 5:3975–3982

[33] Wang Y, Meng L, Fan L, Ma L, Qi M, Yu J, Huang Y (2014) Enhanced interfacial properties of carbon fiber composites via aryl diazonium reaction "on water". Appl Surf Sci 316:366–372

[34] Hao L, Peng P, Yang F, Zhang B, Zhang J, Lu X, Jiao W, Liu W, Wang R, He X (2017) Study of structure-mechanical heterogeneity of polyacrylonitrile-based carbon fiber monofilament by plasma etching-assisted radius profiling. Carbon 114:317–323